29th Congress of the International Council of the Aeronautical Sciences
St. Petersburg, Russia; September 7-12, 2014

THE AERODYNAMIC DESIGN OF THE A350 XWB-900 HIGH LIFT SYSTEM

Henning Strüber*
*** Aerodynamic Design – High Lift Devices,**
Airbus Operations GmbH, Airbus-Allee 1, 28199 Bremen

Keywords: *A350 XWB-900, High Lift, CFD, Wind Tunnel Test, Flight Test*

Abstract

The A350 XWB-900 is the first member of the new family of Airbus long range high-lift aircraft. The development was launched in 2006 and the first aircraft performed its maiden flight in June 2013.

"Shaping Efficiency" was the directive for the design of the aircraft, which was valid for all involved disciplines but of special motivation for aerodynamics. That means for the high-lift system to deliver maximum aerodynamic efficiency for low approach speeds and low take off drag, while keeping the overall system small and simple to provide low weight and low complexity.

1 Design History

In spring 2006 Airbus decided to stop the development of the initial A350, which was based on the A330 in order to offer the customers an all-new aircraft with even better performance, e.g. higher cruise Mach number and aerodynamic efficiency (L/D).

The new clean-sheet design was named A350 XWB, where Extra Wide Body (XWB) referred to the modified fuselage cross-section. The new design should provide a 25% reduction in fuel efficiency compared to its current long range competitors. This was achieved with a new wing layout with more wing sweep allowing for a cruise Mach-number of 0.85. The highly tapered inboard loaded wing is optimized for aerodynamic cruise efficiency and low structural weight. It has been designed in a fully integrated process including aerodynamics, loads and structures. A new high bypass ratio engine is contributing to the low fuel burn, as well as the low weight of the airframe, which was achieved by applying modern materials like Carbon Fiber Reinforced Plastic (CFRP).

The A350 XWB-900 is the baseline layout of a family concept, which foresees also a stretched (-1000) and a shrinked version (-800), see Fig. 1. The -900 accommodates 315 passengers in a typical two class layout, providing a range of up to 7750 nautical miles. The maximum take-off weight is 268 tonnes.

Fig. 1. Airbus A350XWB aircraft family.

Due to the work done already on the initial A350 and the challenging time scales, the concept phase of the A350 XWB was significantly shortened. The milestone, representing the end of the concept phase [1], took place in summer 2006 and the configuration development phase finished with the critical design review (CDR) in summer 2008. Thus the overall aircraft design had to be frozen in two years' time, which was a challenging task not only for the aerodynamics departments.

Enabling was on the one hand the consequent use of efficient design tools like 3D CAD systems and state of the art CFD codes, but also because of the traditionally high engagement of Airbus aerodynamics design departments in research projects. The focus was here on projects dealing with the multidisciplinary design of unconventional high-lift devices. Those activities paved the way for selecting and assessing novel high-lift concepts in an efficient and multidisciplinary way as candidates for the A350 XWB.

2 The high-lift system as an enabler to achieve aircraft design targets

A light weight high-lift system with minimum complexity was requested, enabling the aircraft to achieve

- an outstanding climb performance during take-off, including hot and high conditions, leading to a low drag requirement
- a low approach speed (CAT D, V_{appr} ≈145kts) for safe approaches, supported by the large wing area leading to a moderate maximum lift (C_{Lmax}) requirement
- good handling qualities (A/C attitude in approach, pitch up characteristics, roll capabilities, etc.)
- favorable wake vortex characteristics
- low airframe noise to reduce impact on airport communities

3 High-lift devices on the A350 XWB-900

The layout of the wing movables is sketched in Fig. 2. The wing leading edge is equipped with a Droop Nose Device (DND) inboard and slats outboard. At the trailing edge two Adaptive Drooped Hinge Flaps (ADHF) are installed, covered by a droop panel and seven spoilers. Two ailerons are located outboard of the flaps.

The aerodynamic design process of the high-lift devices is presented in the following chapters.

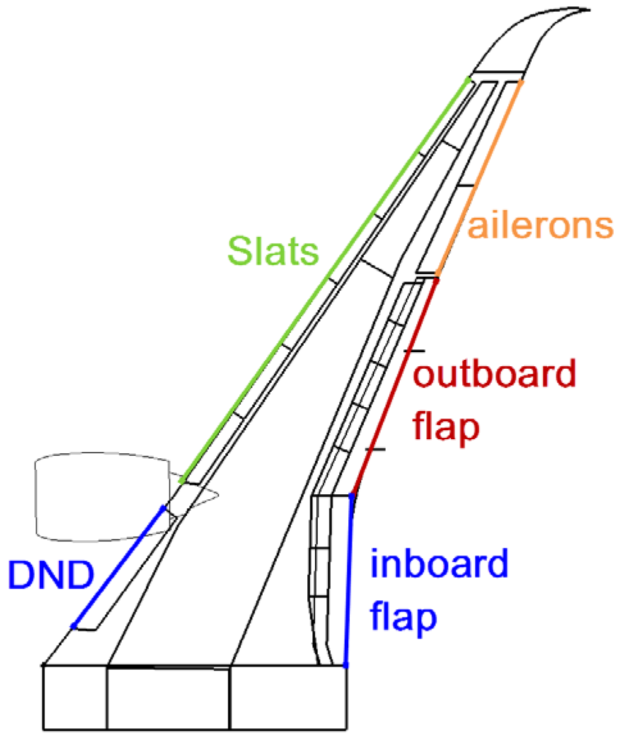

Fig. 2. – A350 XWB-900 wing movable planform.

3.1 Low drag leading edge devices

The main purpose of leading edge devices is to protect the high-lift wing at high angle of attack (α) against too early flow separation, meaning to shift the α_{max} and subsequently C_{Lmax} to higher values. This is achieved by deploying the device and by that reducing the local angle of attack and is further increased by opening a slot between the leading and the trailing element. A detailed description of aerodynamic effects in high-lift is given in [2] and [3].

A vented design solution is well suited to achieve C_{Lmax} targets for landing configurations, but is contradictive to keep the drag of a take-off configuration low. Also the noise emission of a vented leading edge device is significantly higher than for an un-slotted solution, see [4].

The selection and design of the A350 XWB-900 leading edge high-lift devices was driven by the requirement to achieve a maximum take-off L/D in the 2nd segment climb. Hence a device type was needed, which provided a low drag level in take-off configuration, but sufficient protection against flow separation in landing to achieve the required C_{Lmax} values, respectively the approach speed targets.

3.1.1 Inboard Wing – the Droop Nose Device

One challenge to solve was the integration of the 118” (≈3m) diameter Rolls-Royce Trent XWB nacelle with the leading edge high-lift devices. The close coupling of engine and pylon to the wing asked for an inboard high-lift device, which allows a close deployed positioning.

The maximum lift capability of the wing is heavily influenced by the engine installation, leading to subsequent flow separation at high incidences. With the installation of a strake at the inboard nacelle, a high energy vortex is introduced to delay the separation towards higher incidences, see Fig. 5 and Fig. 17.

It was found that a Droop Nose Device (DND) is a good choice for application on the inboard wing leading edge from aerodynamic and integration point of view. The large wing chords in the inner wing region lead to low local lift coefficients. By deploying a DND, the local angle of attack is reduced far enough, to delay the stall. A typical pressure distribution over a wing section with DND can be found in Fig. 3. A moderate suction peak is followed by the characteristic second suction peak with approximately the same c_p level. Compared to a slat, the drag and also the noise level of a DND is much more favorable.

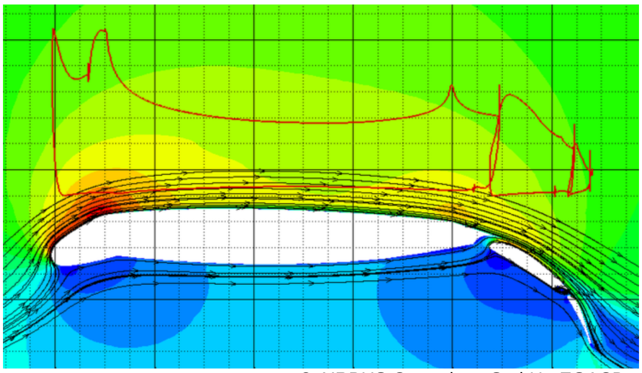

Fig. 3. 2D pressure distribution along a Droop Nose Device (DND) equipped wing.

The DND in combination with the engine installation leads to favorable stalling mechanism, where the inboard wing stalls, while the flow over the outboard wing shall still be attached and the roll control surfaces are not yet affected by the stall. An undesired pitch up behavior of the aircraft, which occurs on highly swept wings when the flow in outboard regions separates, is avoided.

The DND movable rotates on a hinge-line close to the wing lower surface, see Fig. 4, while the movable trailing edge seals against the D-nose surface. Lever arms are rotating the movable, actuated by a drive shaft transmission system to a maximum deployment angle of 25°. A slat would have had more fowler motion at similar deflection angle, which would have made the integration with the engine pylon more challenging.

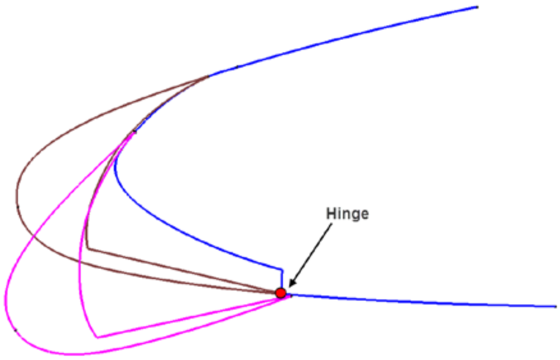

Fig. 4. Droop Nose Device (DND) design principle

During the design process the inner DND-end was cut back to provide room for system components installation. From that cut back resulted an unprotected inner wing leading edge, which is now designed with a fixed droop to avoid early flow separation without compromising the high speed characteristic. Thus the weight and complexity of the DND could be reduced with only minor impact on low speed aero performance. The final arrangement of the DND on the inboard wing leading edge is shown in Fig. 5.

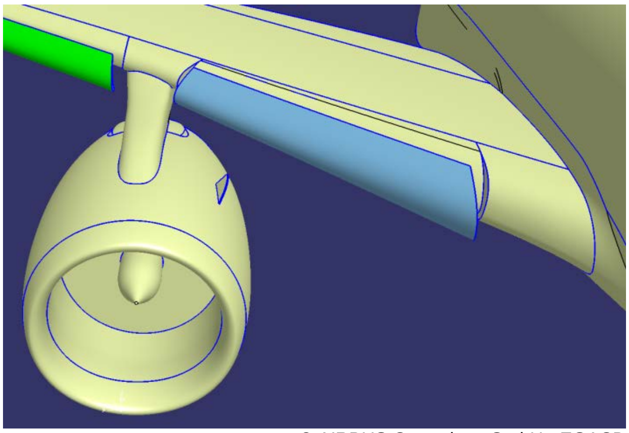
© AIRBUS Operations GmbH - EGACD

Fig. 5. Droop Nose Device installed on the wing

A DND has also been selected on A380 for the inboard wing leading edge, see [10].

3.1.2 Outboard Wing – Sealed Slat

For the outboard wing leading edge a DND seemed to be attractive too, in order to keep the drag of the aircraft as low as possible to achieve the requiered climb performance during take-off. The requirement for sufficient role authority demanded for protection of the outboard wing against flow separation, which could only be achieved with a slat concept.

Although with careful optimization a low drag level can be obtained with a conventional vented slat, a sealed slat was selected to be even more drag efficient. At take-off deployment angle, the slat trailing edge seals against the main wing nose. This keeps the drag level low, but compromises the C_{Lmax} performance in that deployment position due to the missing slot. However, the C_{Lmax} levels reached with the sealed slat in take-off were acceptable and thus no additional protection like e.g. an auto-slat function, as mentioned in [5], was developed.

The C_{Lmax} values achieved in maximum (landing) deployment position are compromised. Due to the choice of the Contour Generated Sealed Slat (CGSS) design method, only little freedom is left to optimize the slat in landing setting. Compared to alternative design approaches like Kinematic Generated Sealed Slats (KGSS) the choice of a CGSS keeps the system complexity and weight low, while the aerodynamic targets are fulfilled, see [6]. The final design of the slat was a compromise between minimum system complexity, low take off drag design with an acceptable impact on C_{Lmax}.

Contour Generated Sealed Slats (CGSS) rotate around a hinge line. The hinge radius is defined by the take-off deployment angle for which the slat trailing edge seals against the main wing D-nose and the desired gap size at landing deployment angle. The design principle is shown in Fig. 6.

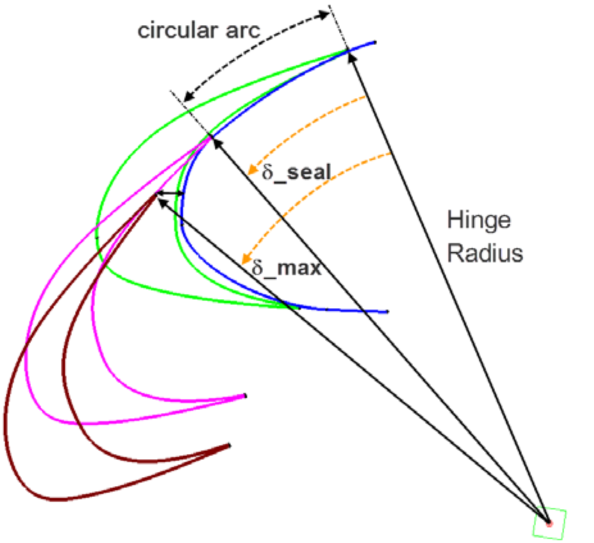

© AIRBUS Operations GmbH - EGACD

Fig. 6. Contour Generated Sealed Slat (CGSS) design principle.

3.2 The trailing edge solution – A multi functional device

For the trailing edge high-lift device a light weight solution with low system complexity was envisaged. However the requirement was given to provide the capability to deploy the flaps independently from each other as variable camber function but also as differential flap setting for load control purposes. This can be applied in early cruise phases to shift the center of lift more inboard and by that reducing the wing root bending moment, which can be transferred into a structural weight saving. In high-lift configuration a more outboard loaded lift distribution can be achieved to reduce induced drag during take-off.

3.2.1 From Research to Product

In the research program HICON a multifunctional trailing edge system has been developed for a short range type transport aircraft. The device was named Slotted Camber

Tab (SCT) and is mentioned in [8]. The spoiler and a lower panel door have been linked mechanically with the flap. The whole system has been designed to be a fast actuated device to merge the primary flight control and the high-lift functionalities, plus a variable camber option to optimize the cruise wing for different loading conditions. The functionalities are illustrated in Fig. 7. At the end of the HICON-project the SCT reached a maturity level, which qualified the concept to be a candidate to be applied on an aircraft.

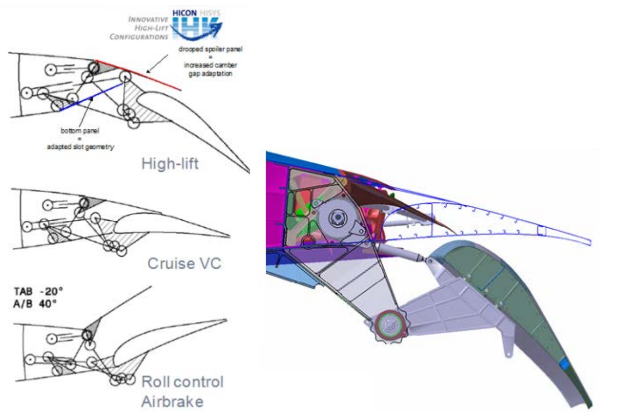

© AIRBUS Operations GmbH – EGACD, ESWTDD

Fig. 7. Hicon SCT and A350 XWB ADHF – multifunctional trailing edge devices in research and product.

3.2.2 The A350 XWB trailing edge high-lift device

The Slotted Camber Tab design has been adapted for the A350XWB to reduce the system complexity and is today known as the Adaptive Dropped Hinge Flap (ADHF). The fast actuation has been dropped, as well as the mechanical link between flap and spoiler. The lower panel door could be designed as a fixed part.

The requested light weight solution with low system complexity was realized by choosing a small flap chord of 19% local wing chord and a hinge kinematic. While flaps deployed on track kinematics enable larger fowler motion (wing area increase) and allow for additional setting optimization for intermediate flap angles (take-off), hinged flaps target a less complex and light weight system architecture, see [6]. However, the drawback is that only one high-lift configuration can be aerodynamically optimized, while the intermediate configurations are a result, as shown in Fig. 8.

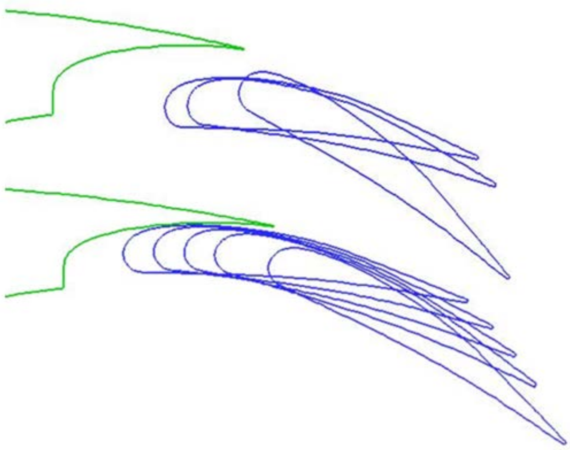

© AIRBUS Operations GmbH - EGACD

Fig. 8. Comparison of Track-Rear-link and hinge kinematics.

Moreover the pivot point needs to be positioned close to the wing in order to minimize the fairing size to limit the impact on cruise drag. By this constraint the fowler motion of hinge flaps is limited.

Another challenge for flaps on hinges is to control the gap between the spoiler trailing edge and the flap, which is essential for attached flap flow. This can be solved by choosing a hinge position close to the wing, which leads to almost no fowler motion of the flap. If fowler motion is desired, the hinge will be much more below the wing. A compromise is to choose a deeper hinge position and to control the resulting large gap with means like a spoiler actuation, which is capable to droop the spoiler when the flap deploys. A flexible spoiler trailing edge as applied on A400M is also a valid solution, see [7]. The most effective mean to reduce the distance between hinge and lower wing surface is to reduce the clean overlap, see Fig. 9, respectively reducing flap chord and/or shifting the shroudline forward. Thus weight of the flap body and support structure is reduced.

The resulting loss in lift can be recovered by applying spoiler droop, which increases the overall camber of the wing, see Fig. 10.

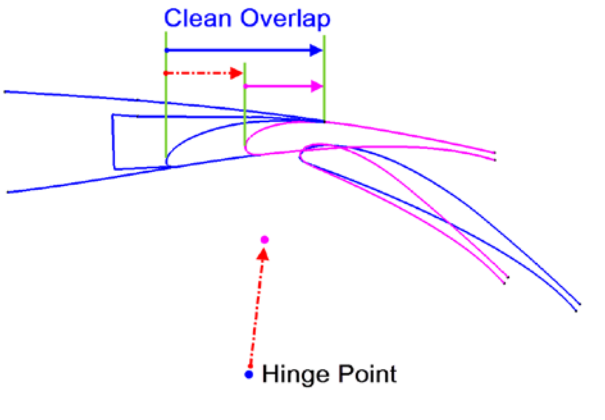

Fig. 9. Effect of reduced flap chord on hinge position at iso flap setting and deployment angle.

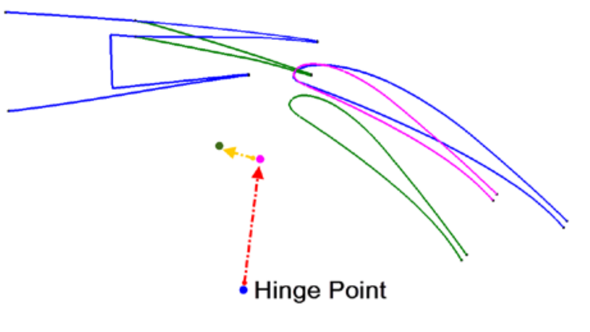

Fig. 10. Effect of applying spoiler droop and higher deployment angle on hinge position at iso flap setting.

The characteristics of the lift polar of a dropped hinge flap with spoiler droop changes compared to the polar of a Single Slotted (Fowler) Flap (SSF) without spoiler droop, see Fig. 11. Due to the additional camber, lift increases in the linear range of the polar. This is favorable for tail strike limited aircraft with long fuselages.

The drawback is a reduced lift slope in the upper non-linear part of the lift polar, which leads to a reduction in maximum lift (C_{Lmax}), see also [11]. This can be recovered by increasing the flap deployment angle of the ADHF, which is possible to a certain extent without separated flap flow due to the help of the drooped spoiler. The higher deployment angle further reduces the distance of hinge point to wing lower surface, while the spoiler droop shifts the hinge point further forward, see Fig. 10.

On the A350 XWB the spoiler actuation is modified to let the spoilers not only deploy as primary flight control device upwards, but also down to 12° to follow the flap when it's deployed on its hinge.

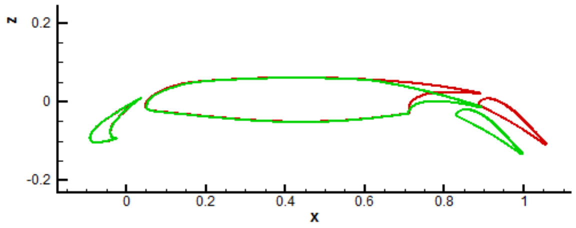

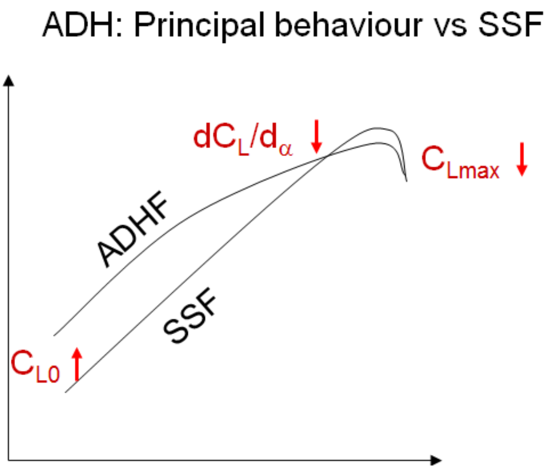

Fig. 11. Effect of applying spoiler droop on lift curve (iso flap deployment angle)

In Fig. 12 a pressure distribution over a flap with and without spoiler droop is shown. Applying spoiler droop changes the pressure distribution: a suction peak can be found on the spoiler leading edge and the pressure at the spoiler trailing edge is increased compared to an un-drooped spoiler. This leads to a reduced spoiler hinge moment at almost constant lift contribution. Overall the load for a high-lift section with spoiler droop is shifted forward on the main wing by the increased rear camber. The resulting higher circulation on the main element reduces the suction peak of the flap due to the increased main element downwash, while the slat sees an increased local angle of attack induced by the local upwash resulting from the main element circulation. By that the slat suction peak is increased.

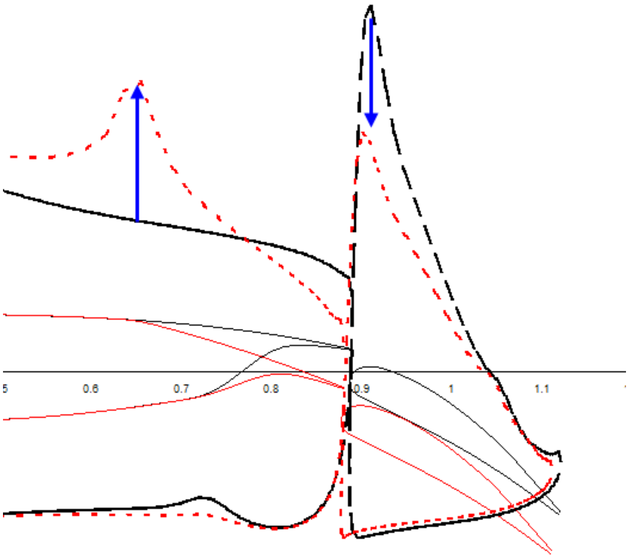

Fig. 12. Pressure distribution over a flap with and without spoiler droop at iso C_L.

3.2.3 Optimizing the trailing edge system

Several design parameters have been varied to find an optimized solution for the ADHF: the chord of flap and spoiler, the chordwise position of the shroudline, the maximum droop of the spoiler and the maximum deployment angle of the flap with its ideal gap and overlap. The main objective was to achieve the given aerodynamic performance targets. An important constraint was to keep the flap hinge close to the wing lower surface in order to minimize the support structure and to keep the size of the flap support fairing, respectively wetted area, low to minimize the impact on cruise drag.

3.2.4 Trailing edge movable layout

Seven Spoilers, two for the inboard flap and five for the outboard flap, are individually actuated and controlled. Only the inner part of the inboard flap is covered by a droop-panel without airbrake functionality. It is mechanically linked with the flap. The movable arrangement is given in Fig. 2.

The inboard flap has an absolute constant chord and is supported on two tracks, where the inner track is located inside the belly fairing. The integration of a new gear beam concept led to a reduction of flap chord of the inner part of the inboard flap, see Fig. 13. Managing the flap gap in this area became even more challenging due to the mechanical linked droop panel, which cannot be actuated independently from the flap deployment.

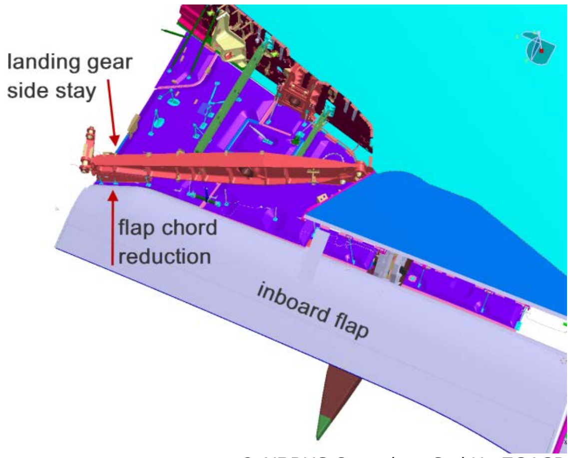

Fig. 13. Landing gear beam integration led to a local flap chord reduction.

The outboard flap has a relative constant chord. It is supported on two tracks and a flap-end-support, which is enclosed inside the wing. It was finally preferred against a three track solution to save weight and friction drag.

Inboard and outboard flap are covering 65% of the wing trailing edge. The remaining wing span is accommodating the inner and outer aileron.

4 The Aerodynamic Design Process

The aerodynamic design process can be divided into several fields of activity: sizing of the high-lift system, device shape design and positioning, design verification by flow simulation and wind tunnel testing, return verification results into design updates and finally validating the aerodynamic performance of the high-lift system in flight test. The aerodynamic design process is embedded into an integrated, multi-disciplinary overall aircraft design process, which finally leads to a product, which is well-balanced between the involved disciplines.

A preliminary sizing of the high-lift system is performed with a semi-empirical tool, which allows a rapid trade of different device types.

The entire shape design process is based on Catia V5, making full use of its parametric and associative capabilities. 3D shapes exist for wing and high-lift devices at any time of the development process.

A customized workbench within Catia exists for high-lift devices design, which allows the designer to introduce and shape rapidly different types of high-lift devices. Design modifications can be efficiently introduced and monitored. The design knowledge has been wrapped into Knowledge Based Engineering (KBE) templates. This allows a highly efficient shape design process and ensures a constant high quality of the resulting 3D shapes.

The workbench also provides interfaces to different 2D Computational Fluid Dynamics (CFD) tools to analyze the aerodynamic characteristics of the designed solutions quickly.

To get optimal flow characteristics, an optimum device setting for a given shape, respectively a combination of gap, overlap and deployment angle must be found. The setting parameters are varied to obtain a response surface of the aerodynamic sensitivities. Two dimensional Reynolds Averaged Navier-Stokes (2D RANS) flow simulations are performed as described in [9] at several spanwise sections. Shape and setting parameters are modified in the 3D Catia model according to the found aerodynamic sensitivities. The aerodynamic performance of that pre-optimised high-lift wing is then verified with 3D RANS CFD. The extensive use of 3D CFD was limited during this development phase due to the compressed timescales in the A350 XWB development.

The KBE tool enabled an iterative design process within six weeks including clean wing modifications for high speed affecting the high-lift devices as well as revised kinematic constraints or requirements. Only the above described efficient process chain enabled the high-lift design team to deliver high-lift devices shapes in time with high quality.

The efficiency of the 3D CFD process has improved significantly in the last years by automating many steps, which were conducted manually before. This enabled an extensive use of 3D CFD after the design freeze in 2008 for e.g. performance and loads data generation, also for specific cases like A/C in ground effect, jet-flap interference and high-lift system failure cases.

5 Wind tunnel testing for A350 XWB

Wind tunnel tests started early in the design phase: a concept half model was put into the Airbus Bremen Low Speed Wind Tunnel (BLSWT) to generally investigate different high-lift concept solutions at the very beginning of the design process. By doing this, several different concepts were compared in an early point in time. It was also valuable to improve the maturity on novel high-lift concepts and allowed a concept down selection on a mature data base.

The model consisted of existing major model components and rapid prototyping high-lift devices, see Fig. 14. The use of a wind tunnel facility operating at atmospheric pressure allowed rapid prototyping to be used extensively to manufacture high-lift devices on short notice and a cost efficient testing. Clearly the effect of the low Reynolds-number (≈1.5e6) had to be taken into account, when using the measured data on aircraft level.

Fig. 14. The early concept model in BLSWT.

Two sets of models were built during the design phase, representing different level of shape maturity. Each model set consisted of a half model and two full model at different scale. They were tested in Airbus facilities and external wind tunnels to generate datasets at low, medium and high Reynolds-number, fulfilling the different requirements of the aerodynamic departments.

6 First Flight and high-lift configuration optimization flight test

The A350 XWB-900 maiden flight took place on 14. June 2013 and lasted 4h, see Fig. 14. Real time telemetry at all airbus sites allowed engineers to follow flight tests and asses the basic aircraft parameters in situ.

Fig. 15. A350 XWB-900 MSN1 first flight on 14. June 2013

The low speed flight test campaign showed satisfying results. Both, take-off drag as well as landing performance turned out to be well on the spot. Thanks to the multifunctional high-lift system the flap flow could be fine-tuned by changing the spoiler droop to control the flap gap, which supported an early high-lift configuration freeze. The pilots can apply different high-lift configurations: a flap-less setting for holding pattern, three take-off and a landing configuration.

The analysis of flight test data, consisting of pressure measurements, flow visualization and global aerodynamic data showed a good match of flow features out of simulation, wind tunnel testing and flight test. The found stalling behavior gives a clear feeling of reaching maximum lift to the pilots including the desired pitch down motion of the aircraft.

6 Conclusion

The aerodynamic design of the high ligft system of the A350 XWB-900 has been presented. The design rationale behind the low drag leading edge devices as well as for the multi-functional trailing edge device was given. The applied aerodynamic design process is described from sizing studies, shape design, design verification in wind tunnel and with CFD and design validation in flight test.

7 Acknowledgement

The author would like to thank his colleagues for the support they provided to write this paper, but also for the years of dedication and fellowship in designing a high-lift system for the 350 XWB aircraft family members. In person: J. Hansing, T. Ehlers, K. Schindler, U. Scholz, A. Eberle, D. Reckzeh, H. Friedel, L. Andreani, S. Tischler.

Contact Author Email Address

mailto: henning.strueber@airbus.com

References

[1] Altfeld, H.-H. *Commercial Aircraft Projects – Managing the development of Highly Complex Products*. 1st edition, Ashgate, 2010.
[2] Smith, A. – *High-lift Aerodynamics* – Journal of Aircraft, Volume12, June 1975
[3] Van Dam, C. P. – *The aerodynamic design of multi-element high-lift systems for transport airplanes* – Progress in Aerospace Science 38 - 2002, page 101-144
[4] Fischer, M.; Sutcliffe, M.; Friedel, H.; Gölling, B. – *Trends for low noise high-lift design derived from wind-tunnel tests.* - ICAS Proceedings 25th congress 2006
[5] Nield, B. N. – *An overview of the Boeing 777 high-lift aerodynamic design* - Aeronautical Journal, November 1995
[6] Rudolph, P. K. C. – *High-lift Systems on Commercial Subsonic Airliners* – NASA Contract Report 4746, September 1996
[7] Reckzeh, D. – *Aerodynamic Design of the A400M High-lift System* – ICAS Proceedings 26th congress 2008
[8] Sutcliffe, M., Reckzeh, D., Fischer, M. – *Hicon Aerodynamics – High-lift Aerodynamic Design for the future* - ICAS Proceedings 25th congress 2006
[9] Schindler, K., Reckzeh, D., Scholz, U., Grimminger, A. – *Aerodynamic Design of High-lift devices for civil transport airctraft using RANS CFD* – Proceedings 28th AIAA conference 2010
[10] Reckzeh, D. – *Aerodynamic design of the high-lift system of a megaliner aircraft* - Aerospace Science and Technology 7, 2003, page 107-119
[11] Valarezo, W. O.; Dominik, C. J.; McGhee, R. J.; Goodman, W. L. – *High Reynolds Number Configuration Development of a High-Lift Airfoil* – AGARD, October 1992

Copyright Statement